

## Record of earthquake phenomena in a Lower–Middle Triassic sedimentary basin (North Sudetic Synclinorium, Lower Silesia, SW Poland)

Karol DURKOWSKI<sup>1, 2, \*</sup>

<sup>1</sup> KGHM Cuprum Research & Development Centre, gen. Wł. Sikorskiego 2–8, 53-659 Wrocław, Poland

<sup>2</sup> AGH University of Science and Technology, Faculty of Geology, Geophysics, and Environmental Protection, Al. Mickiewicza 30, 30-059 Kraków, Poland



Durkowski, K., 2022. Record of earthquake phenomena in a Lower–Middle Triassic sedimentary basin (North Sudetic Synclinorium, Lower Silesia, SW Poland). *Geological Quarterly*, 66: 38, doi: 10.7306/gq.1670

Deposits of the Röt Formation (Lower–Middle Triassic) in the eastern part of the North-Sudetic Synclinorium (Bolesławiec Syncline), SW Poland, include numerous synsedimentary deformation structures. Six boreholes with a total core length of ~434 m enabled macroscopic analysis and description of these deformation structures, supplemented by borehole log interpretation, calcimetric analysis, and interpretation of 2D surface seismics. An interval up to ~42 m-thick at the base of the Röt Formation showed both brittle and soft-sediment deformation structures. Their abundance and intensity decrease towards the top of the Röt Formation, and they completely disappear in the Muschelkalk (Middle Triassic). Both the number of boreholes and their locations indicate the presence of such structures across the entire study area. The occurrence of deformation structures in each borehole analysed and their large lateral range suggest that the uppermost part of the Lower Triassic and lowermost part of the Middle Triassic in the study area were influenced by seismic activity. As a result, tectonic reorganization of the study area is inferred for the latest Early/earliest Middle Triassic.

Key words: seismites, tectonic activity, brittle deformation, soft sediment deformation structures, boreholes.

### INTRODUCTION

Recognition of soft-sediment deformation structures in Triassic provides critical information on an event or events that occurred during or shortly after sedimentation. Alongside soft-sediment deformation structures there co-occur brittle deformation structures, which are equally numerous at the same stratigraphic level. The main difference between them is that soft-sediment deformation structures are commonly found in fine clastic deposits (siltstones, claystones). In contrast, brittle deformation structures occur primarily in carbonate strata (limestones, dolomites). Their distribution can be related to the lithological variability in the Röt Formation. Many events can contribute to the formation of soft-sediment deformation structures, ranging from bioturbation, gravitational instability, gravitational collapse caused by dissolution, storms, rapid and sudden sediment deposition, to earthquakes, and these processes can also contribute to the formation of brittle deformation structures.

Seismic waves are a potential cause of such a deformation style. The term seismite is used to describe deformation structures formed in sedimentary rocks due to earthquakes and the secondary seismic waves (S-waves) so generated (Seilacher, 1969; Allen, 1982, 1986). Seismites have been described in nu-

merous publications, e.g. Seilacher (1969), Casagrande (1976), Allen (1982, 1986), Wojewoda (1987), Owen and Moretti (2008), Moretti and Van Loon (2014). Earthquakes are most commonly linked to tectonic phenomena involving stress accumulation and release via fault formation, but may also be associated with processes such as mass movements, meteorite impacts, or glacio-isostatic rebound loading (Belzyt and Pisarska-Jamroży, 2017). Identifying earthquakes as the cause of deformation is possible by eliminating alternative phenomena (Seilacher, 1984; Wojewoda and Burliga, 2008). If the structures analysed form a correlative horizon over a large area, then they may be an indicator of seismic shaking – seismites (Wojewoda, 2008). The pattern of deformation produced by an earthquake is determined by factors such as the type of lithology and its variability, the degree of porosity and fluid filling of the sediment, the degree of packing of the sediment and its compactness (e.g., Seilacher, 1969; Allen, 1986; Wojewoda, 2008; Moretti and Van Loon, 2014; Belzyt and Pisarska-Jamroży, 2017). The interpenetration of two types of deformation at the same levels is determined by lithology and the susceptibility of lithology to the rate and degree of cementation.

This paper describes the second occurrence of such deformation structures recognised in the succession of the Bolesławiec Syncline. Similar structures were recognised and described in the siliciclastic deposits from the Permian/Triassic boundary interval (Durkowski et al., 2017). They were also noted in the Middle Triassic (Muschelkalk) of the Silesia–Kraków and Holy Cross Mountains area (Szulc et al., 2015;

\* E-mail: karol.durkowski@kgghmcuprum.com

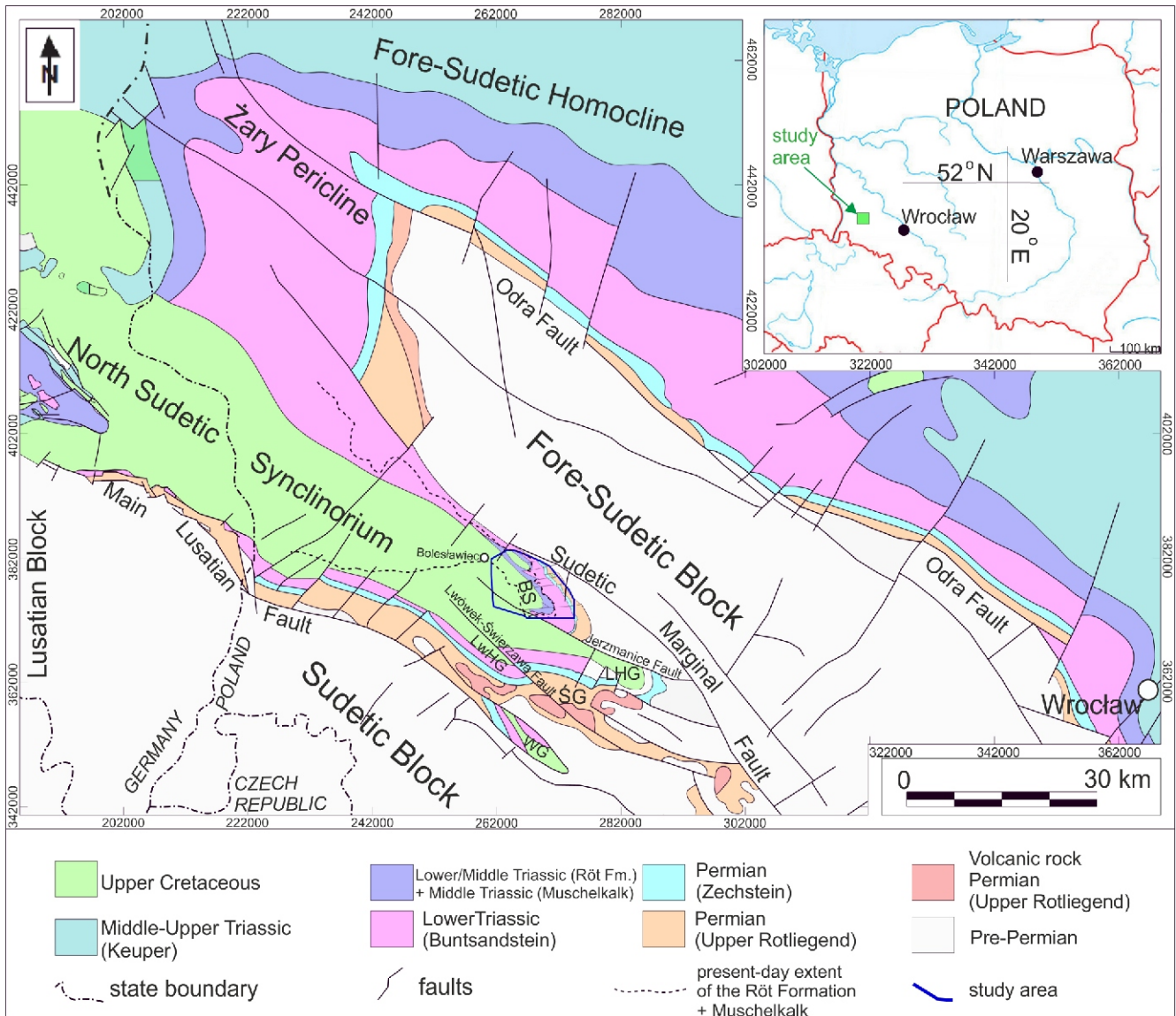


**Fig. 1. Location of the study area on a geological map**

BS – Bolesławiec Syncline; ŚG – Świerzawa Graben; LHG – Leszczyna Half-Graben; LwHG – Lwówek Śląski Half-Graben; map after (Dadlez et al., 2000, modified <http://m.bazagis.pgi.gov.pl/cbdg>; Hielscher and Hartsch, 2010, modified)

Matysik and Szulc, 2019). Syndepositional and early post-depositional deformation structures have never been described from the uppermost Lower Triassic and Middle Triassic of the North Sudetic Synclinorium. Therefore, this research aims to demonstrate the tectonic activity and its variability in the study area during the sedimentation of the Röt Formation. It is suggested that secondarily-developed seismic phenomena may have been a direct cause of syn-sedimentary deformation in the Röt Formation deposits.

## GEOLOGICAL SETTING

The study area is located in southwestern Poland, in the northern part of the Sudetic Block (Żelaźniewicz and Aleksandrowski, 2008; Żelaźniewicz et al., 2011) and eastern part of the North Sudetic Synclinorium, within a smaller (secondary) unit known as the Bolesławiec Syncline (Fig. 1; Krasoń,

1967). In its early development, the North Sudetic Synclinorium constituted a NW–SE aligned intermontane basin and was one of the main regions of sediment accumulation in the systematically uplifted Sudetes area (Wojewoda and Mastalerz, 1989). The North Sudetic Synclinorium represents a structure formed due to the evolution of a sedimentary basin that had developed during the Carboniferous-Permian in the northern Sudetic foreland (Sokołowski, 1967; Milewicz, 1968; Wojewoda and Mastalerz, 1989; Raczyński et al., 1998; Śliwiński et al., 2003; Solecki, 2011). According to most studies (e.g., Sokołowski, 1967; Bałazińska and Bossowski, 1979; Solecki, 1994; Śliwiński et al., 2003; Żelaźniewicz et al., 2011; Głuszyński and Aleksandrowski, 2021), the Laramian Phase (Alpine orogeny) was the main stage of evolution of the North Sudetic Synclinorium and the Bolesławiec Syncline. The unit is WNW–ESE oriented, and its axis plunges to the NW. The outlines of the North Sudetic Synclinorium and Bolesławiec Syncline are shown in Figure 1.

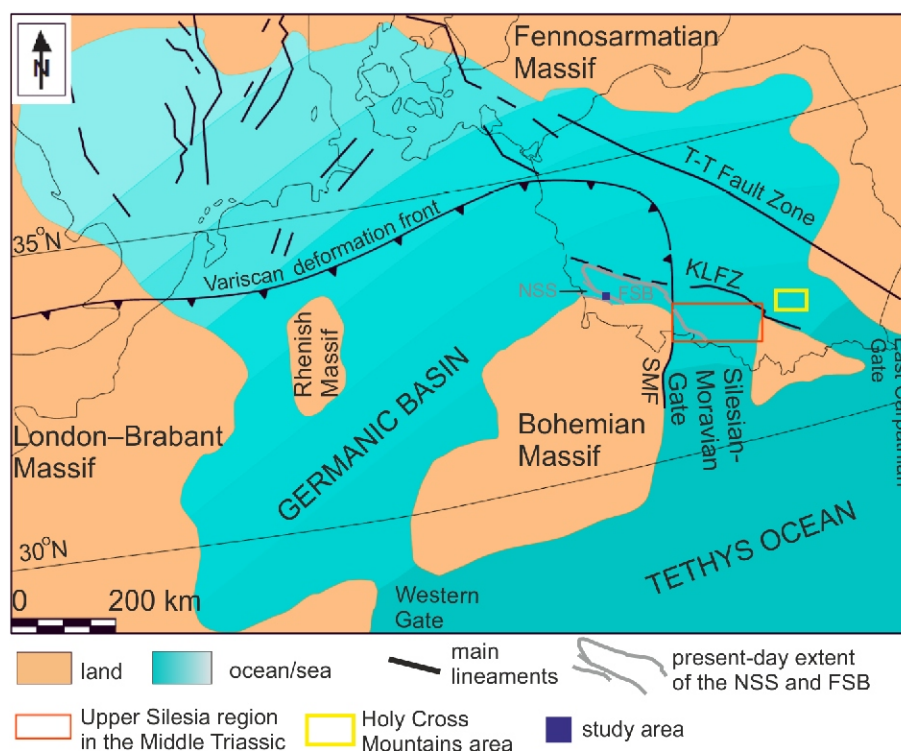


**Fig. 2. Palaeogeographic position of the North Sudetic Synclinorium (NSS) and the Fore-Sudetic Block (FSB) in the Middle Triassic**

KLFZ – Kraków–Lubliniec (Hamburg) Fault Zone; T-T Fault Zone – Teisseyre-Tornquist Fault Zone; SMF – Silesian–Moravian Fault; N – Triassic North; map modified (Matysik and Szulc, 2019)

During the Early Triassic, the area of the North Sudetic Synclinorium represented a small part of the southern margin of the Germanic Basin (Fig. 2). The Germanic Basin was an epicontinental basin connected during the latest Early Triassic with the Tethys Ocean through the Silesian-Moravian and Eastern Carpathian gateways (Fig. 2; e.g., Bachmann et al., 2010; Szulc, 2010; Matysik and Szulc, 2019). From the middle Anisian, the Western Gate also became active (Fig. 2; e.g., Szulc, 2010; Matysik and Szulc, 2019).

The sedimentary-volcanogenic succession of the North Sudetic Synclinorium comprises upper Carboniferous to Upper Cretaceous deposits, with a stratigraphic gap encompassing the Upper Triassic, Jurassic, and Lower Cretaceous. The succession overlies the lower Paleozoic metamorphic basement (Raczyński et al., 1998).

This study is focused on the Upper Buntsandstein (Röt Formation), i.e. the uppermost Lower Triassic and lowermost Middle Triassic deposits of the Bolesławiec Syncline (Milewicz, 1985; Szyperko-Teller and Moryc, 1988; Senkowiczowa, 1992; Bachmann et al., 2010; Cohen et al., 2013).

The facies, sedimentology, and fauna of the Röt Formation and Muschelkalk in the North Sudetic Synclinorium have been studied mainly by Milewicz (1962, 1971, 1985), Sokołowski (1967), Leśniak (1978), Szyperko-Teller and Moryc (1988), Raczyński et al. (1998), Chrząstek (2002), and Chrząstek and Wojewoda (2011). The tectonic structure in the study area and its vicinity was discussed by Sokołowski (1967), Milewicz (1968, 1976, 1977), Bałazińska and Bossowski (1979), Leśniak (1979), Cymerman (1998) and Solecki (2011).

Extent, thickness and distribution of the Röt and Muschelkalk deposits in the Bolesławiec Syncline

Triassic carbonates (Röt Formation+Muschelkalk) occur in the study area in a NW–SE oriented belt (Fig. 3). Its width varies from ~4.5 to ~2.7 km and its length is ~14 km (Fig. 3). The largest thicknesses of Triassic carbonates in the study area occur both in its northern and southeastern parts (Fig. 3). The Röt Formation and Muschelkalk reach maximum thicknesses of 465.3 m (Fig. 3; historic borehole W-37). The closest borehole in which the subdivision into the Röt Formation and Muschelkalk has been made is W-1/1. Triassic carbonates reach 353 m in thickness, with the upper Röt Formation attaining a thickness of ~207 m and the Muschelkalk 146 m. In turn, in the southeastern part of the area, the Triassic carbonate strata reach a thickness of ~240.0 m (based on the isopachs shown in Figure 3; in the nearest borehole G-2, the Röt Formation reaches a thickness of 100.5 m, and the Muschelkalk 104.0 m).

## MATERIAL AND METHODS

The study is based on data from 19 boreholes drilled between 2011 and 2016 (termed “new boreholes” below), lithostratigraphic descriptions of ~60 boreholes drilled in the 1940s–1980s (“historic boreholes”) and surface 2D seismic studies made in 2016. All boreholes were drilled to document the Permian sediment-hosted copper deposit. 2D seismics and well logs were carried out to investigate the geological and mining conditions of the study area. All archival geological samples, including borehole cores, were destroyed in the early 1990s. All new boreholes and 2D seismic from 2016 were commissioned by KGHM Polska Miedź S.A. All data from

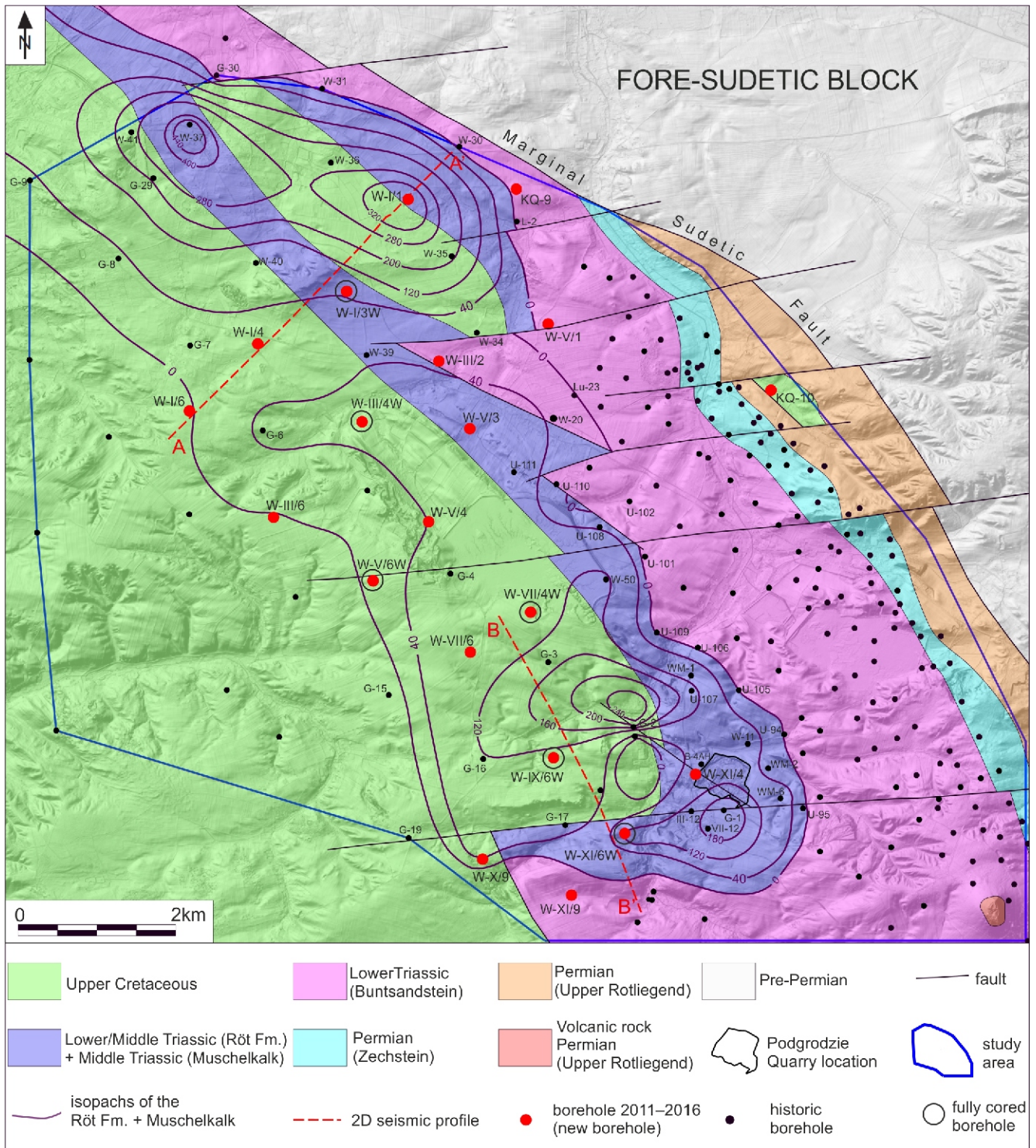
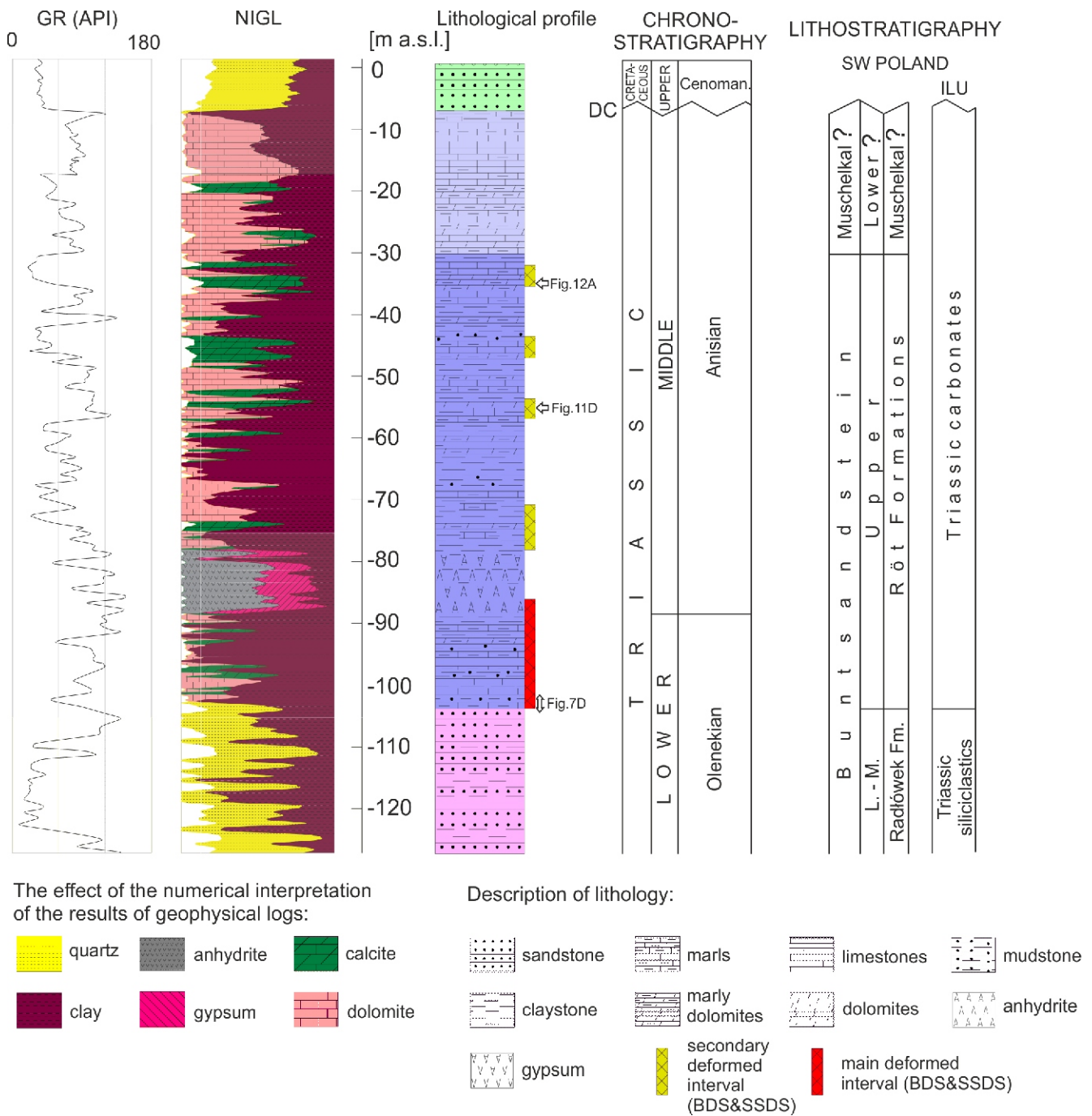


Fig. 3. Detailed geological map of the study area, without Cenozoic (after Dadlez et al., 2000, modified; Głuszyński et al., 2019, modified)

2011–2016 are the property of KGHM Polska Miedź S.A. and the Ministry of Climate and Environment and are not publicly available according to law.

Among the 19 new boreholes, 6 were fully cored (W-I/3W, W-III/4W, W-V/6W, W-VII/4W, W-IX/6W, W-XI/6W), whereas in 2 additional boreholes (W-III/2; W-VII/6) the core was collected only from selected sections of the Triassic. In the remaining 11 boreholes, geological samples of Triassic carbonates are represented by cuttings. A total of ~4798 m of core was collected

from the Triassic, out of which ~434 m represents Triassic carbonates. The lithological descriptions and lithostratigraphic subdivisions in the new boreholes were carried out by the author. Based on macroscopic core observations, calcimetric analysis determining the  $\text{CaCO}_3$  and  $\text{CaMg}(\text{CO}_3)_2$  content, and interpretation of well logs, the lithological column of the Röt Formation and Muschelkalk was prepared (Figs. 4 and 5). The minerals visible on the geophysical profile are the result of numerical interpretations from geophysical logs. The lithological com-



**Fig. 4. Generalized lithostratigraphic column of the Röt Formation and Muschelkalk, borehole W-IX/6W 238.7 m a.s.l.**

GR – Gamma Ray Logging; NIGL – numerical interpretation of the results of geophysical logs; ILU – Informal Lithostratigraphic Units; DC – Disconformity; BDS – brittle deformation structures; SS DS – soft-sediment deformation structures (chronostratigraphy after Cohen et al., 2013; SW Poland lithostratigraphy after Milewicz, 1985; Śliwiński et al., 2003; cf. Petrovic and Aigner, 2017)

position of the rocks present in the well logs was assessed using Interlog software. The following measurement curves were used for interpretation with Interlog: GR, NPFI, CNT, BCS, SGR, CDL, MSFL and DLL. The lithostratigraphic subdivision was also established based on studies in which the faunal content of the Röt Formation and Muschelkalk was analysed (Leśniak, 1978; Chrzastek, 2002). Additionally, to verify the lithostratigraphic subdivisions, cores from boreholes W-XI/6W and W-IX/6W were compared with the exposed succession in Podgrodzie Quarry in Raciborowice Górne (Fig. 3). Only ~35 m of the topmost part of the Muschelkalk and >10 m of the Röt Formation are exposed in that quarry.

The isopachs of Triassic carbonates were based on lithological columns of new and historic boreholes (Fig. 3). Additionally, 2D seismic data and well logs recorded at the same time were also used in this paper. Lack of subdivision or lack of subdivision criteria into the Röt Formation and Muschelkalk in some historic boreholes and the need to use these data resulted in the presentation of the combined isopachs for the Röt Formation and the Muschelkalk under the term Triassic carbonates (Fig. 3). These informal subdivisions refer only to the study area. They are aimed at characterising, presenting and distinguishing deposits formed in aqueous settings.

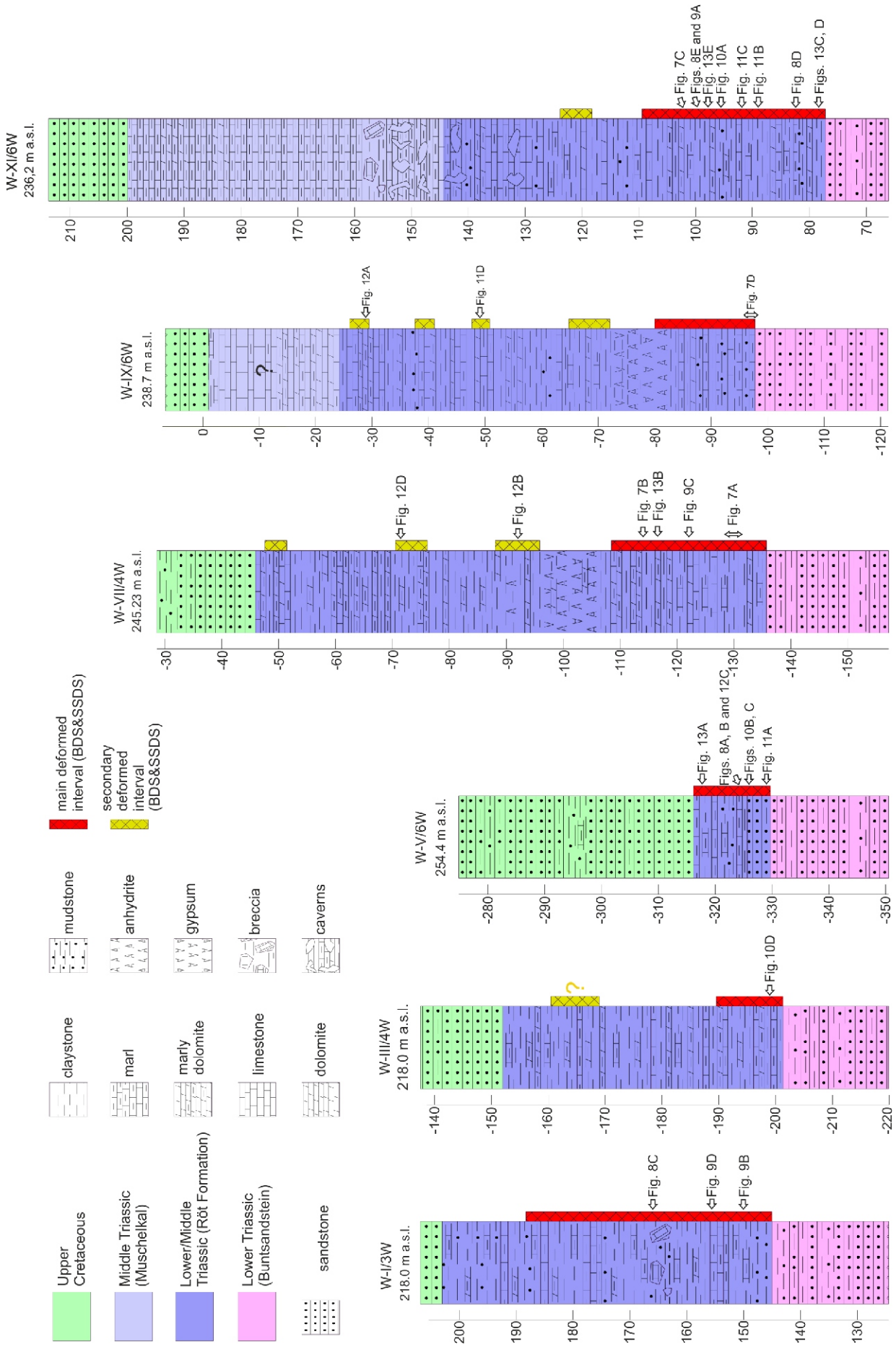


Fig. 5. Generalized lithostratigraphic columns of the Röt Formation and Muschelkalk with intervals of brittle and soft-sediment deformation structures

BDS – brittle deformation structures; SSDS – soft-sediment deformation structures

2D seismic data was made, processed and interpreted by Geopartner Sp. z o.o. (Miluk et al., 2016). Later, the seismic profiles in the depth domain were subject to reinterpretation using the Petrel suite of Schlumberger. These interpretations were performed by Andrzej Głuszyński and Karol Durkowski for another study in preparation. For the needs of this paper, 2 out of 23 available seismic profiles are illustrated (Fig. 3). 2D seismic data allowed visualisation of the occurrence of the Röt Formation and Muschelkalk strata with regard to the underlying Lower and Middle Buntsandstein, as well as to determine the orientation and geometry of faults (Fig. 6).

Interpretations of deformation structures occurring in the Röt Formation were made based on macroscopic observations of borehole cores. Deformation structures are present in all six fully-cored boreholes (for borehole locations, see Fig. 3). The classification of deformation structures was based on similar structures distinguished in the study area and the Wleń Graben area in strata across the Permian/Triassic boundary and in the Silesia-Kraków area in the Middle Triassic (Durkowski et al., 2017; Kowalski et al., 2018; Matsyk and Szulc, 2019).

## RÖT FORMATION AND MUSCHELKALK IN THE BOLESŁAWIEC SYNCLINE

### LITHOLOGICAL LOG

The Röt Formation overlies the homogeneous, red-brown sandstones and conglomeratic sandstones representing the undivided Lower and Middle Buntsandstein. The Röt Formation is represented by alternating claystones, marls, marly mudstones, mudstones, marly limestones, dolomitic limestones, and locally calcareous dolomites. The carbonate interbeds are usually from ~10 cm to ~1.5 m-thick, and light-grey to grey in colour. The fine-grained deposits are black-grey and green-grey of various shades. The large lithological variation is emphasised by sharp boundaries and occasionally erosional surfaces. The carbonates contain numerous intraclasts, usually semi-rounded to semi-angular, from several millimetres across to ~4 cm long, ellipsoidal, rarely discoidal or spindle-shaped. The intraclasts are represented by green-grey and black-grey claystones.

Additionally, a sulphate horizon was recognised at the base of the Röt Formation (e.g., Fig. 4). Gypsum and anhydrite, representing the sulphate horizon, are characterised by a variable clay content and are grey to pink, rarely white-grey in colour. Sulphates were noted only in 8 of the boreholes studied (W-I/1, W-VII/6, W-VII/4W, W-IX/6W, G-2, G-3, G-16, G-1). The sulphate thickness varies from ~2 to 16 m.

Borehole W-V/6W was unique as directly above the weathered middle Buntsandstein, in the base of the Röt Formation, there are grey, strongly disturbed sandstones ~3 m-thick (Fig. 5). This is the only documented occurrence of Röt Formation sandstones in the study area.

In the N and SE part of the study area, Röt deposits pass gradationally into the Muschelkalk, which was distinguished only in boreholes G-1, G-2, W-I/1, W-XI/6W, W-IX/6W, and in Podgrodzie Quarry. This unit is represented by beige and grey dolomitic and marly limestones. The limestones alternate with greyish-black clayey marls and marls, and are highlighted by planar and flaser lamination. The thickness of the laminae varies from a few millimetres to several centimetres. Intervals with caverns and breccia are located in the base of the Muschelkalk, as distinguished in borehole W-XI/6W (Fig. 5). Such intervals were also observed in Podgrodzie Quarry. The breccia noted is associated with the secondary filling of caverns and possibly also their gravitational collapse.

## BRITTLE AND SOFT-SEDIMENT DEFORMATION STRUCTURES

Brittle deformation structures can be defined as a permanent change that occurs in a solid material due to the growth of fractures and/or due to sliding on fractures (van der Pluijm and Marshak, 2004). The term “brittle deformation structure” can refer to deformation style and microscale deformation mechanisms (Haakon, 2010). Brittle deformation occurs only when stresses exceed a critical value, and thus only after a rock has already undergone some elastic and/or plastic behaviour (van der Pluijm and Marshak, 2004). Brittle deformation structures observed in borehole cores are represented by reverse faults, normal faults, neptunian dykes, injection dykes and autoclastic breccia.

Soft-sediment deformation structures (SSDS) arise when liquified, hydroplastic, and sometimes more competent sediments are stressed during or shortly after deposition (Allen, 1982). We can define SSDS as any deformation structure, other than vertical compaction, of sediment or sedimentary rock that is achieved by rearrangement of the original sedimentary particles, without internal deformation of those particles or any interstitial cement (Waldron and Gagnon, 2011 after Maltman, 1984, 1994b). Deformation occurs primarily through grain-boundary sliding (Waldron and Gagnon, 2011). SSDS include liquefaction and fluidization structures, load structures, convolute bedding, and deformation structures related to rockfalls.

The thickness of levels with deformation structures varies from ~10 m (borehole W-III/4W) to ~42 m (borehole W-I/3W). The layers with deformation structures are mainly located at the base of the Röt Formation, where they represent almost the entire deformed interval – the main deformed interval (Figs. 4 and 5). Undeformed layers within such intervals have thicknesses from over ten to several tens of centimetres and are irregular (Fig. 7A–C). The lower boundary of the main deformed interval is represented by sandstone of the Buntsandstein (Fig. 7D). The top of the main deformed interval cannot be unequivocally attributed to any lithological boundary. Nevertheless, in two boreholes (W-VII/4W and W-IX/6W) it is capped by a sulphate unit (Figs. 4 and 5). In the remaining cored boreholes, sulphate beds were not observed; therefore the relation of the intervals with deformation structures to sulphates cannot be determined. However, above the main deformation interval in borehole W-XI/6W there is an accumulation of clay, which probably represents the equivalent of the sulphate unit (Fig. 5). Brittle deformation structures and SSDS also occur above the main deformation interval, but they are very rare, restricted to beds with a thickness from several tens of centimetres to ~3 m, and much less spectacular (secondary deformed intervals). In this case, the thickness of the undeformed intervals separating the occurrences of particular deformation structures is usually several metres and more.

A unique case was observed in borehole W-III/4W. Two intensely deformed intervals were noted there: the first interval at the base of the Röt Formation, ~10 m-thick, and the second at the top of the Röt Formation, ~6 m-thick (Fig. 5). The thickness of the undeformed interval separating the occurrences of those two deformation levels is 20 m. It cannot be excluded that the two separate deformation intervals are in fact related to duplication of the Röt Formation strata. So far, over a dozen repetitions of beds within the Zechstein, and Lower and Middle Buntsandstein have been recognised by the author's personal observations. Therefore, such repetitions can also be expected within the Röt Formation. In borehole W-V/6W, the entire 13.2 m of the Röt Formation is deformed. This borehole is lo-

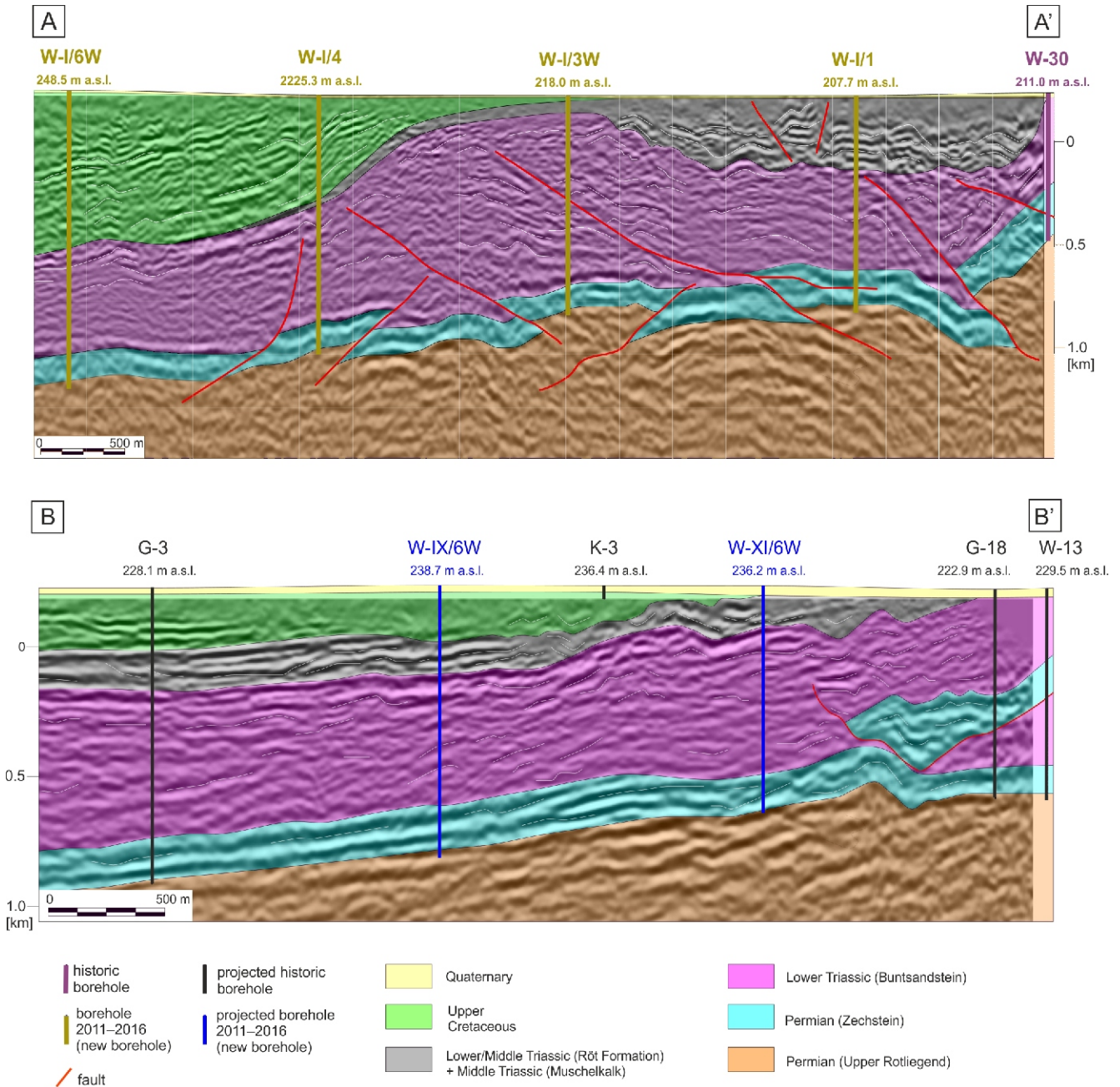


Fig. 6. 2D seismic cross-section (after Miluk et al., 2016, modified; Głuszyński et al., 2019, modified)

cated in the south-western part of the Triassic carbonates' distribution where the recognised units are thin (Fig. 5). Borehole W-V/6W is characterised by a large number of folds, liquefaction, and fluidization phenomena, and convolute bedding.

Generally, neither type of deformation structure was observed in the Muschelkalk, which is represented mainly by limestones and dolomites alternating with marls and clay marls.

BRITTLE DEFORMATION STRUCTURES

SMALL-SCALE FAULTS

Core-scale reverse and normal faults are relatively common features in the cores analysed. The shift of beds on the fault plane varies from several millimetres to ~10 cm. In a few cases,

the faults cut the entire core diameter and thus their origin cannot be stated clearly (Fig. 8E). The fault surfaces are adjacent to one another. In some cases, the detached rock layers are separated by a space which is at most 2 millimetres thick and filled with clay.

Normal faults are usually related to the liquefaction of the underlying deposit and collapse of the overlying strata (Fig. 8). Reverse faults and overthrusts are also accompanied by evidence of sediment instability. Compression may be linked with liquefaction and flow of clastic material under high pressure and, as a result, the impact of rocks more susceptible to fracturing during deformation. It may also be linked with substrate instability and the resulting stress. Reverse faults, rarely overthrusts, are often noted in the vicinity of folds and convolutions. Depending on the lithology, part of the sediment is frac-



**Fig. 7. Deformation structures in selected core sections**

**A** – brittle and soft sediment deformation structures, borehole W-VII/4W (depth 374.0–377.0 m); **B** – brittle (BDS) and soft sediment deformation structures, borehole W-VII/4W (depth 358.0–359.0 m); **C** – brittle deformation structures (BDS), borehole W-XI/6W (depth 133.0–134.0 m); **D** – an example of the transition from sandstone of the Buntsandstein (bottom of the photo) to the Röt Formation (top of the photo), borehole W-IX/6W (depth 340.0–343.0 m)

tured, whereas the other, more susceptible, part is subject to plastic deformation (Fig. 8B, D). This phenomenon is favoured by different lithologies and different thicknesses.

#### NEPTUNIAN DYKES

Neptunian dykes are a relatively rare feature in the cores analysed. Usually, the fractures are up to 1 cm in diameter and from several to over ten centimetres deep (Fig. 9). There is one case in which the fracture diameter is close to the core diameter, i.e. ~9 cm; in this case its depth reaches almost 30 cm (Fig. 9C; borehole W-VII/4W). The interior of the fracture, formed in dolomitic limestone, has sharp edges and is filled with the overlying clay. Lithoclasts of the host rock are observed at the top and base of the fracture (Fig. 9).

Neptunian dykes represent fractures formed in a cemented sea-bottom deposit (Allen, 1982; Smart et al., 1988; Matyszkiewicz et al., 2016; Matysik and Szulc, 2019). Fractures formed on a cemented sea-bottom deposit may be caused by

tectonic extension, unstable escarpments, sediment uplift and bulging, and develop a long time before being filled with sediment (Allen, 1982). Neptunian dykes are usually filled with sediment showing rhythmic lamination and that may contain lithoclasts of the host rock (Matysik and Szulc, 2019).

#### INJECTION DYKES AND AUTOCLASTIC BRECCIA

Injection dykes (Fig. 10) and accompanying autoclastic breccia are present in almost every borehole. To some extent, the diameter of the core hampers observations. Only some structures are small enough to be captured in the core (Fig. 10A, D). In some cases, despite their small dimensions, the observed structures run obliquely to the core axis and are partially preserved. Structures which are preserved only partially, due to their size or shape or relation to the core axis, were assigned to injection dykes and autoclastic breccia based on their characteristic features (Figs. 8C and 10B, C).

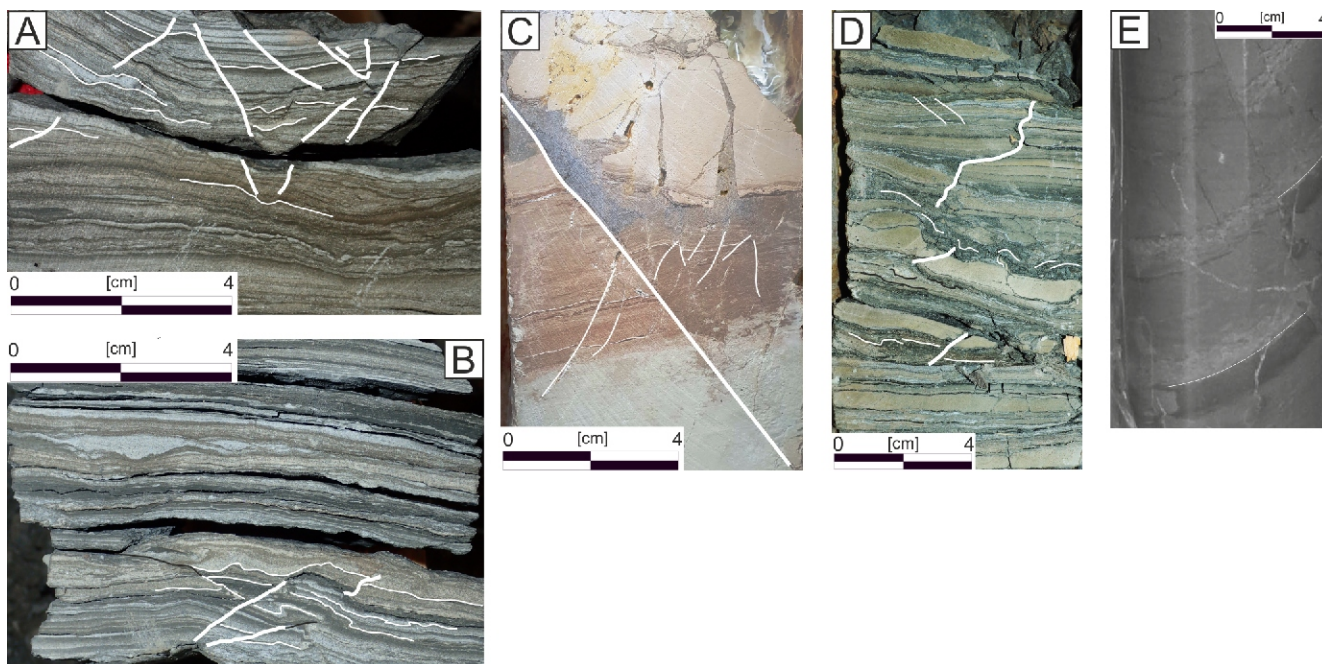


**Fig. 8. Brittle deformation structures**

**A** – syndepositional normal faults, alternations of marly limestone, marl and mudstone, borehole W-V/6W (depth 579.6 m); **B** – overthrusts, reverse faults and folds, alternations of marly limestone, marl and mudstone; load structures visible in upper part of photograph, borehole W-V/6W (depth 579.8 m); **C** – normal fault, note a series of secondary reverse and normal faults in the hanging wall and footwall, note autoclastic breccia in upper part of photograph, borehole W-I/3W (depth 44.8 m); **D** – syndepositional reverse fault, borehole W-XI/6W (depth 156.4 m); **E** – reverse fault, note complementary fractures in lower part of photograph, borehole W-XI/6W (depth 136.7 m)

Injection dykes are structures formed during change in the rheology of a rock medium that is oversaturated with water (Sibson et al., 1975; Kämpf et al., 1985; Labaume et al., 2004; Wojewoda and Burliga, 2008). Therefore, the formation of such structures is characterised by increase in pore pressure, contributing to fracture opening and intrafractional flow of fluidised material (Wojewoda, 2008; Wojewoda et al., 2016; Durkowski et al., 2017). Moreover, injection dykes are characterised by sharp boundaries and sinking intraclasts of undeformed sediment, resembling breccia and often forming jigsaw-puzzle patterns in which particular fragments match each other (Wojewoda, 2008; Matysik and Szulc, 2019).

#### SOFT SEDIMENT DEFORMATION STRUCTURES (SSDS)

The largest accumulation of soft-sediment deformation structures (SSDS) was observed in the lowermost part of the Röt Formation, a similar pattern to that of the brittle deformation structures. They are also observed higher in the succession, but in much smaller numbers.

#### LIQUEFACTION AND FLUIDIZATION STRUCTURES

Liquefaction structures (Fig. 11) are a common phenomenon in the cores analysed. They display a variable degree of fluidisation and deformation, which has a variable impact on the surrounding deposits. Fluidisation structures are a rare phenomenon in the study area; only a few examples were observed (Fig. 11C). Liquefaction and fluidisation structures occur both in the carbonate and marly-mudstone interbeds (Figs. 10B, C and 11B–D). Usually, they represent core-scale small structures. In individual cases, the structures have dimensions larger than the core diameter. For example, the sandstones from the base

of the Röt Formation in borehole W-V/6W represent the most spectacular case of liquefaction structures (Fig. 11A). The entire 3 m thickness of the sandstones is affected by liquefaction.

According to the author's observations, both liquefaction and fluidisation structures may also be interpreted as a process or stage leading to the formation of autoclastic breccia, injection dykes, load structures or convolutions. Nevertheless, numerous observations indicate the presence of liquefaction and fluidisation phenomena without visible impact on the over- or underlying deposits (Fig. 11C, D). Therefore, liquefaction and fluidisation structures may be defined as deformation structures which have stopped at a certain stage and thus have not evolved into other secondary structures. Consequently, these phenomena are assigned to deformation structures herein.

As with injection dykes, liquefaction and fluidisation structures are formed due to rapid pore pressure increase in a medium oversaturated with water (Sibson et al., 1975; Kämpf et al., 1985; Labaume et al., 2004). They are thus related to the flow of solutions under high pressures, liquefaction of the sediment, its deformation and fluid escape (Allen and Banks, 1972; Lowe, 1975; Matysik and Szulc, 2019). In the case of liquefaction structures, the fluid source is within the bed; therefore deformation should be uniform in the entire deformed unit (Lowe, 1975; Matysik and Szulc, 2019). Fluidisation structures are local phenomena related to upwards fluid flow under pressure from the lower-lying beds (Lowe, 1975; Matysik and Szulc, 2019).

#### LOAD STRUCTURES

In the initial part of liquefaction and sinking of the overlying, more dense material, ball and pillow structures are formed (Fig. 12A). Usually, they represent fragments of the sediment

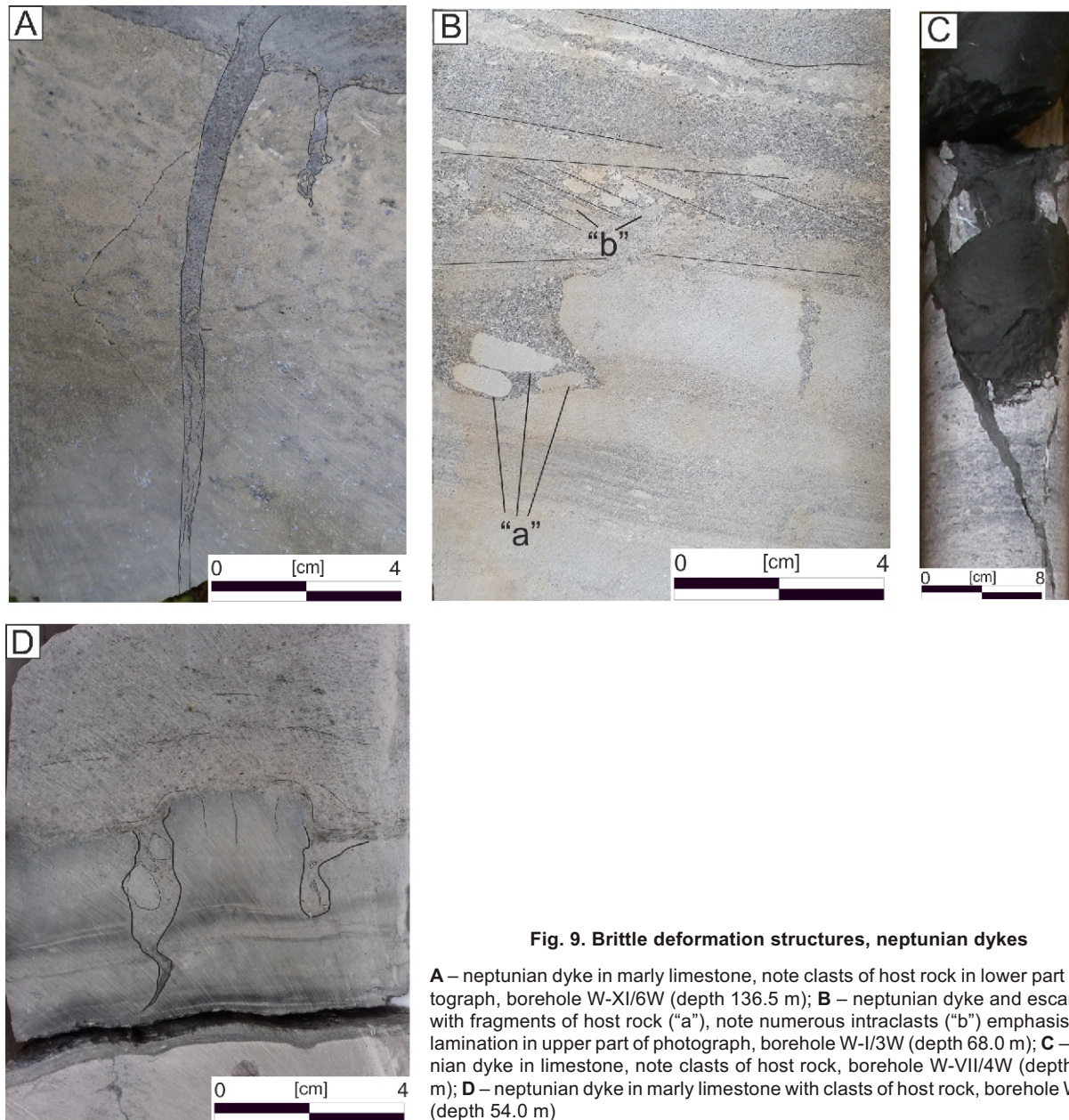


**Fig. 9. Brittle deformation structures, neptunian dykes**

**A** – neptunian dyke in marly limestone, note clasts of host rock in lower part of photograph, borehole W-XI/6W (depth 136.5 m); **B** – neptunian dyke and escarpment with fragments of host rock (“a”), note numerous intraclasts (“b”) emphasising the lamination in upper part of photograph, borehole W-I/3W (depth 68.0 m); **C** – neptunian dyke in limestone, note clasts of host rock, borehole W-VII/4W (depth 369.0 m); **D** – neptunian dyke in marly limestone with clasts of host rock, borehole W-I/3W (depth 54.0 m)

that lost connection with the overlying host layer and attained oval and spherical forms or concave-up synclines (Kuenen, 1965; Gradziński et al., 1986). In the cores analysed, the load structures present are characterised by the overlying sediment “b” having the properties of a brittle body, as shown by its fracturing and sinking into the underlying sediment (Figs. 10B, C and 12C). The structure represents an autoclastic breccia but without fractures and intrafractional flows. The underlying sediment “a” is partly fluidised, although faults and overthrusts can often occur within it (Fig. 12C). Sediment “a” is frequently deformed with its internal structure partly or completely obliterated (Fig. 12B).

Load structures may be formed both in fresh, unconsolidated sediments as well as due to deformation of the underlying sediments, this being linked with liquefaction and fluidisation processes and structures. Unstable density lamination in the „ba” system develops in this case (Gradziński et al. 1986). In such a system, layer “b” with a larger bulk density is located above layer “a” with a smaller bulk density. An increase in pore pressure and liquefaction of sediment “a” may cause equilib-

rium instability and fracturing of the overlying sediment “b”, followed by its sinking in the form of angular fragments. When the overlying sediment is unconsolidated or fluidised, fragments of the deformed overlying sediment sink into the sediment with a lower density (Kuenen, 1965; Anketell et al., 1970). When pore pressure decreases, the process of load structure formation may be stopped at any moment, resulting in the preservation of various stages of deformation (Fig. 12D).

#### CONVOLUTE BEDDING

Convolute bedding is a rare feature in the cores analysed, occurring in only two of them. The largest amount of such structures was observed in borehole W-V/6W, and one example was noted in borehole W-VII/4W. Usually, the deformed layers are several centimetres thick (Fig. 13A, B). They are represented by alternations of mudstone and marly limestone, each with a thickness of several millimetres, which show plastic deformation.

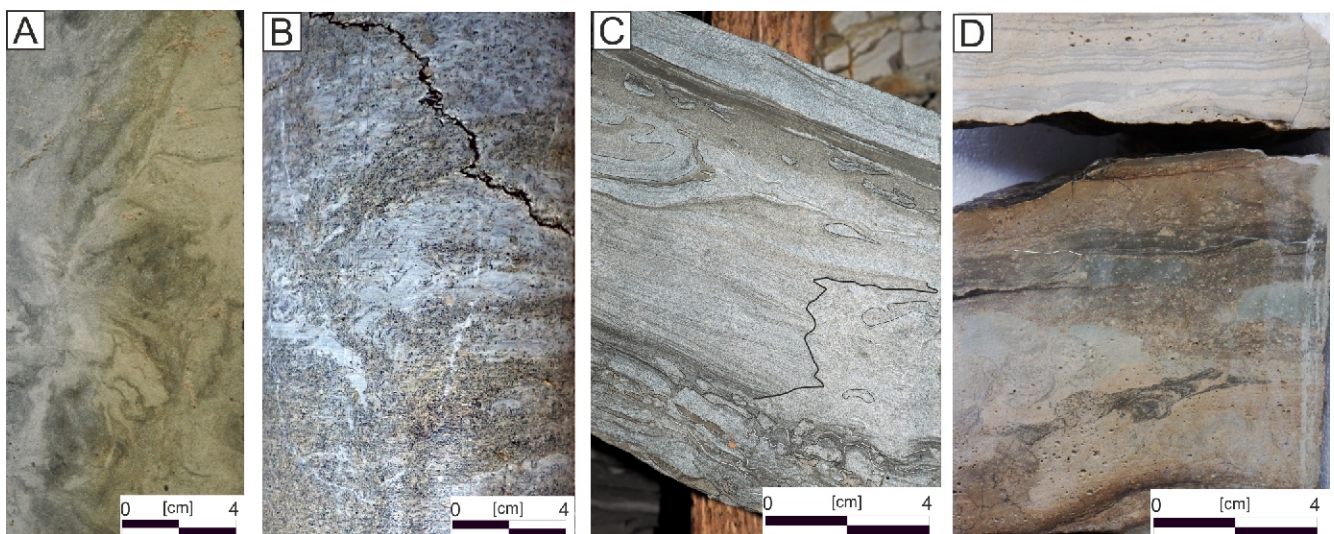
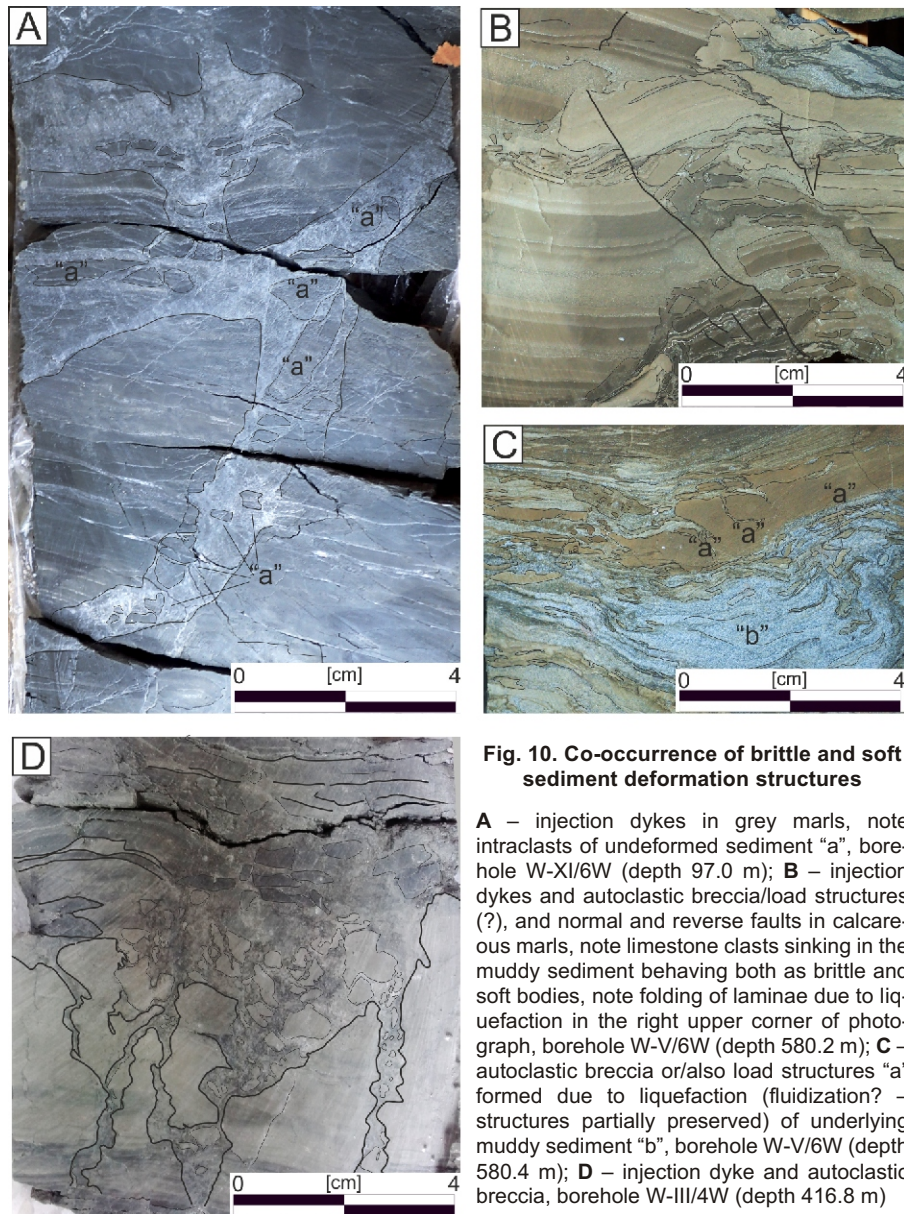


**Fig. 11. Soft sediment deformation structures (SSDS)**

**A** – liquefaction structures in greenish-grey sandstone, borehole W-V/6W (depth 583.0 m); **B** – liquefaction structures in bioclastic limestone, note layers of light grey limestone that were subject to fluidization and deformation, borehole W-XI/6W (depth 86.6 m); **C** – fluidization structures in mudstone, note disruption of layer of beige limestone in the lower right corner of photograph, note single load structure, borehole W-XI/6W (depth 141.9 m); **D** – liquefaction structures in marly limestone, note disruption of greyish-black lamina in upper part of photograph, borehole W-IX/6W (depth 294.4 m)

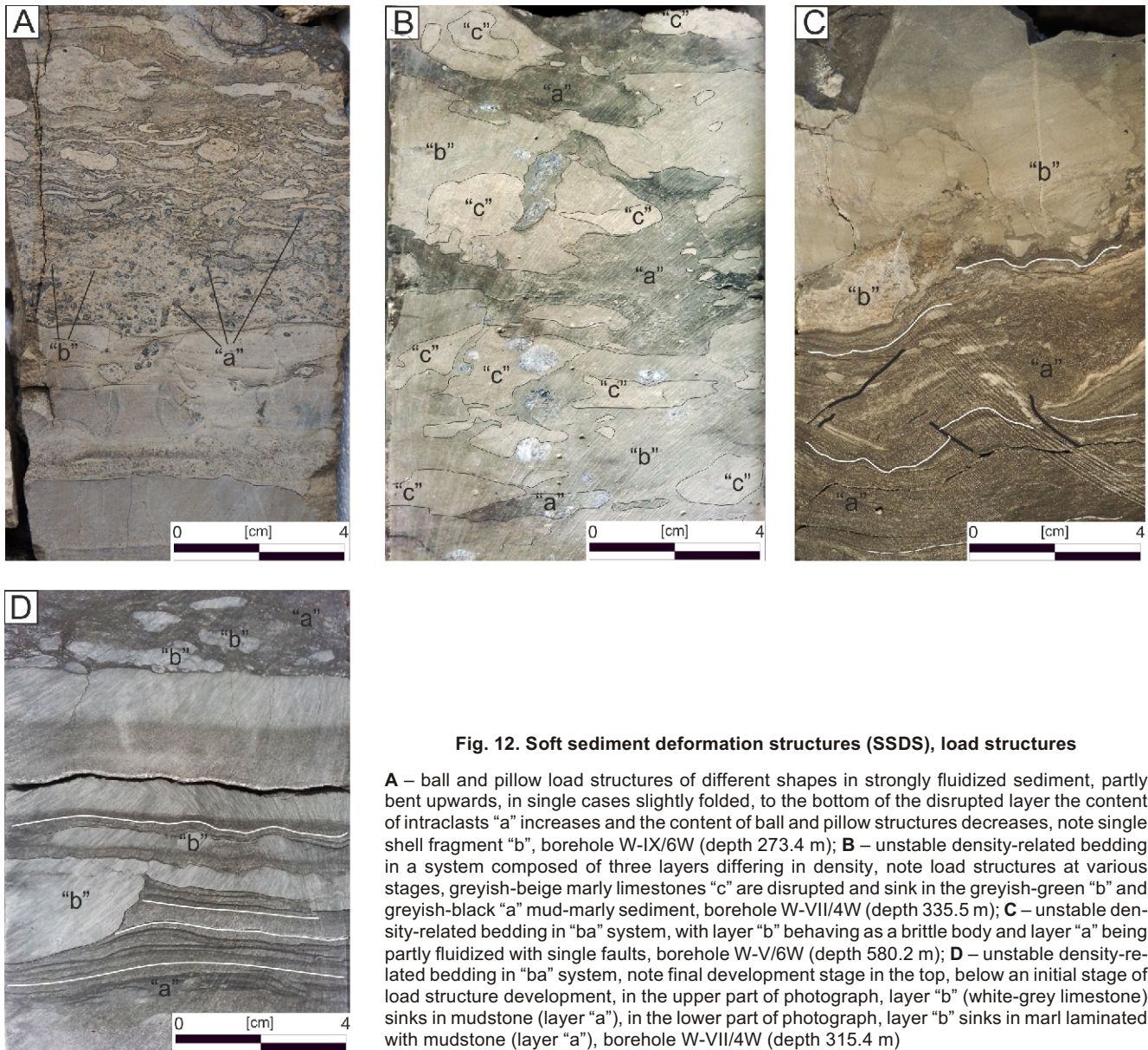


**Fig. 12. Soft sediment deformation structures (SSDS), load structures**

**A** – ball and pillow load structures of different shapes in strongly fluidized sediment, partly bent upwards, in single cases slightly folded, to the bottom of the disrupted layer the content of intraclasts “a” increases and the content of ball and pillow structures decreases, note single shell fragment “b”, borehole W-IX/6W (depth 273.4 m); **B** – unstable density-related bedding in a system composed of three layers differing in density, note load structures at various stages, greyish-beige marly limestones “c” are disrupted and sink in the greyish-green “b” and greyish-black “a” mud-marly sediment, borehole W-VII/4W (depth 335.5 m); **C** – unstable density-related bedding in “ba” system, with layer “b” behaving as a brittle body and layer “a” being partly fluidized with single faults, borehole W-V/6W (depth 580.2 m); **D** – unstable density-related bedding in “ba” system, note final development stage in the top, below an initial stage of load structure development, in the upper part of photograph, layer “b” (white-grey limestone) sinks in mudstone (layer “a”), in the lower part of photograph, layer “b” sinks in marl laminated with mudstone (layer “a”), borehole W-VII/4W (depth 315.4 m)

Convolute bedding represents the internal deformation of laminae in the form of different folds, in which the lamina shortening reaches 50% at the preservation of layer thickness (Gradziński et al., 1986). Usually, horizontal lamination occurs below and above the deformation structures, and the passage from deformed laminae to undeformed laminae is gradual. The genesis of convolute bedding is an intricate process and cannot be explained with one simple diagram or definition (Gradziński et al., 1986). For example, these structures form either when the sediment is deposited on a gentle slope (Leeder, 1999; Collinson et al., 2006) or during the escape of water from the sediment and the resulting increase in pore pressure (Gradziński et al., 1986).

#### DEFORMATION STRUCTURES RELATED TO ROCKFALLS

Deformation structures related to rockfalls are a rare feature in the cores analysed, occurring in only one borehole (W-XI/6W). The inclusion of deformation structures related to rockfalls in the SSDS is primarily related to the deformation of soft sediment by falling consolidated rock fragments (Matysik and Szulc, 2019). They are represented by semi-angular,

beige-grey marly limestone fragments with maximum dimensions of 10 x 6 cm, which in many cases cause substrate deflection (Fig. 13C, D). In the core scale, it is extremely difficult to recognise rock-fall-related deformation. Only by analogy with similar structures observed in Upper Silesia (Matysik and Szulc, 2019) and through the determination of other structures in the succession described can it be suspected that the rock fragments observed represent this process.

Sediment deformation structures caused by falling fragments of rocks have been described by numerous authors (e.g., Wallace, 1984; Amit et al., 1995; Matysik and Szulc, 2019). Usually, these structures are related to gravitational rockfall near escarpments and other irregularities in the sedimentary basin.

#### DISCUSSION

A characteristic feature of the described deformation structures is their prevalence in the lowermost part of the Röt Formation and their gradual disappearance towards the top of this unit. Another important issue is the co-occurrence of brittle and

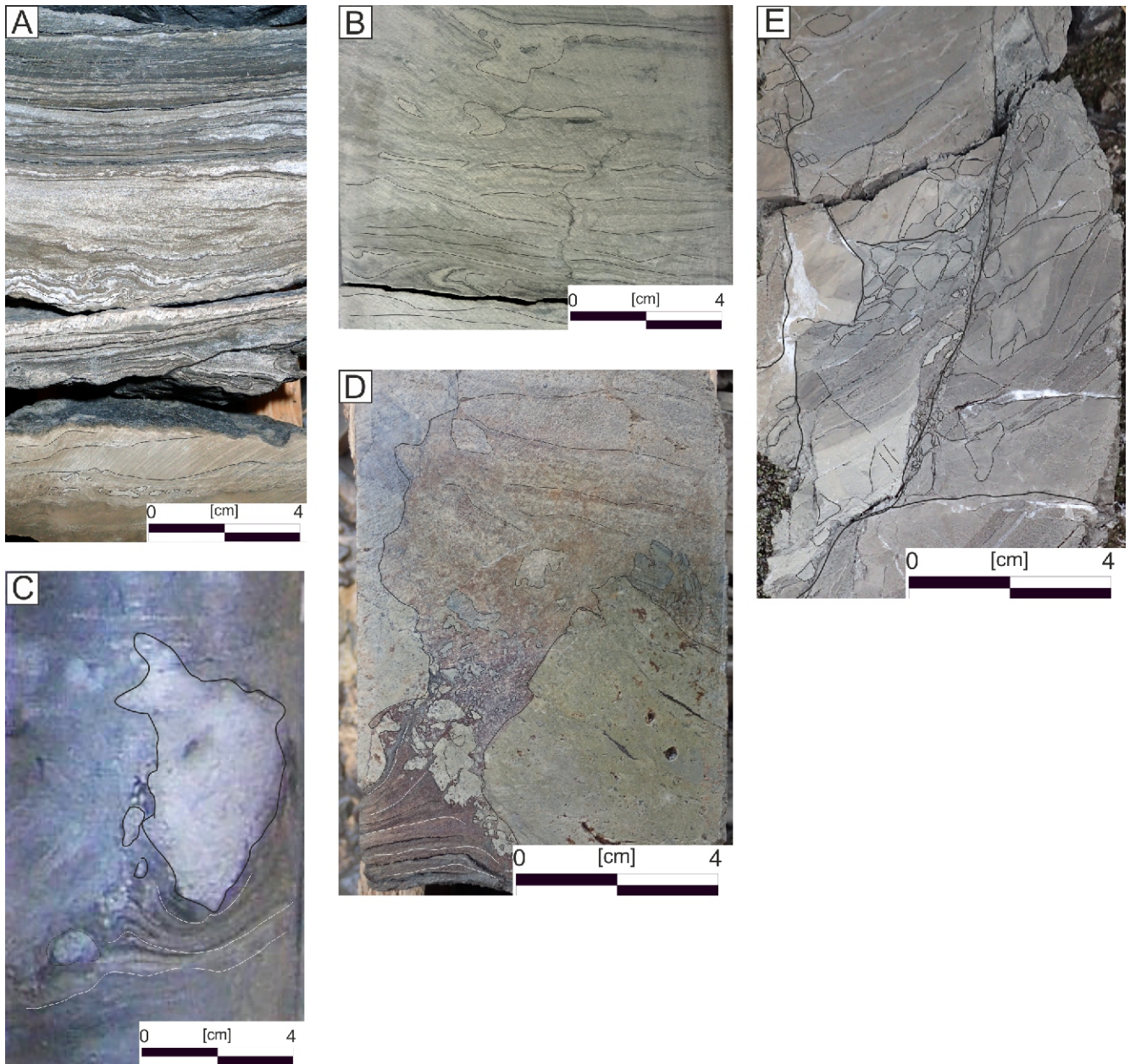


**Fig. 13. Soft sediment deformation structures (SSDS) and an example of large scale tectonic structure**

**A** – convolutions of calcareous-mud sediment, borehole W-V/6W (depth 572.8 m); **B** – convolutions in lower part of photograph, load structures in upper part of photograph, borehole W-VII/4W (depth 363.2 m); **C** – deformation structures related to rockfalls, base deflected, borehole W-XI/6W (depth 158.8 m); **D** – deformation structures related to rockfalls, borehole W-XI/6W (depth 158.0 m); **E** – part of large-scale tectonic structure, borehole W-XI/6W (depth 137.2 m)

soft-sediment deformation structures. The Muschelkalk is characterised by lithological homogeneity and a lack of such brittle and soft-sediment deformation structures. This has been shown by borehole and exposure data (i.e., Podgrodzie Quarry in Raciborowice Górne). Therefore, the Middle Triassic was probably characterised by a seismic quiescence within the study area.

Depending on the lithology, contribution of clastic material, saturation of the rock mass, solution flow, or the presence of forces such as cohesion, brittle deformation structures may develop simultaneously with soft-sediment deformation structures (Gradziński et al., 1986; Fossen, 2010). Fine clastic sediments (siltstones, claystones) are more susceptible to the develop-

ment of SSDS than are carbonates (limestones, dolomites). The reason for this may reflect that fine-grained sediments are more heterogeneous and more water-saturated than are carbonates. On the other hand, cementation usually occurs more rapidly in carbonates (Gradziński et al., 1986; Matysik and Szulc, 2019). In the event of an earthquake, the pore pressure increases in sediments that are more saturated with water. An increase in the pore pressure promotes sediment plasticisation or brittle deformation (Gradziński et al., 1986). The presence of brittle deformation structures in the study area points to partial consolidation of the deposits as the forces were applied.

The presence of particular deformation structures sandwiched between undeformed deposits, the variety of defor-

mation structures and the lack of slickensides or open fractures allow postulation of their syndepositional origin (Rupke, 1978; Gradziński et al., 1986; Belzyt and Pisarska-Jamroży, 2017). Sandwich-like structures can be also described as the sedimentary contact of deformed and undeformed sediments (Fig. 7). The brittle deformation structures noted above can be also determined as being of early post-depositional origin (Anketell et al., 1970; Allen, 1982; Kastens, 1984; Gradziński et al., 1986; Hampton et al., 1996). Sediment liquefaction may occur at depths of as much as 5–10 m (McCalpin and Nelson, 2009; Belzyt and Pisarska-Jamroży, 2017). On the other hand, Shao et al. (2016) demonstrated sediment liquefaction at depths of 2–5 m, where the thickness of the liquefied sand was 2 m. Those sediments were examined at a distance of 3 km from the earthquake epicentre. Allen (1986) has shown that sediment liquefaction with a potential for SSDS development may be induced at sites as far away as 700 km from the epicentre of an M 7.5 earthquake (Shanmugam, 2016). A much smaller lateral extent of deformation (e.g., 20–113 km) was suggested by e.g. Papadopoulos and Lefkopoulos (1993), Kirkland and Anderson (1970) and Kirkland et al. (2000). The spatial distribution and lateral changes of seismites are much more complex than a simple relationship between the earthquake and the large lateral extent of earthquake-related deformation (Alfaro et al., 2010; Rodríguez-Lopez et al., 2007; Shanmugam, 2016).

The deformation structures discussed occur at the transition from continental facies (Lower and Middle Buntsandstein) to shallow marine facies (Röt Formation). The reverse transition in lithology and sedimentary environment (marine to continental settings) coupled with similar deformation structures was also observed at the Permian/Triassic boundary (Durkowski et al., 2017; Kowalski et al., 2018). The uppermost Permian deposits are represented by mudstones and very fine-grained sandstones (heterolithic deposits), which pass into typical red-brown Triassic sandstones. Most probably, transgression and change of the sedimentary setting were controlled by tectonic processes, e.g. tectonic movements related to the activation or reactivation of the Fore-Sudetic Block (?). Interpretations of rock mass movements in the Fore-Sudetic Block area, e.g. in the uppermost part of the Permian (Rotliegend), were given by Bałazińska and Bossowski (1979), on the basis of a lack of Rotliegend deposits in the Bolesławiec N-24 borehole located a few kilometres to the NW of the study area in the vicinity of the Fore-Sudetic Block. On the other hand, the occurrence of deformation structures in the Röt Formation may have resulted from a single tectonic event which caused gravity-driven mass wasting. In this case, the shifting rock masses, and the resulting stress and strain, would directly cause brittle and soft-sediment deformation structures (Potter and Pettijohn, 1963; Anketell et al., 1970; Rupke, 1978; Allen, 1982; Gradziński et al., 1986; Hampton et al., 1996; Masson et al., 2006). Gravitational mass movements may have occurred after the deposition of the Röt Formation. In the case of gravitational mass movements, sediment deformation depends on many factors, including lithology, its variability, and the compactness of individual sediments. The seismic process would rather be a secondary cause of the deformation. The largest deformation structures at the base of the Röt Formation and their gradual disappearance can be explained by the nature of the gravitational movements. At the base of the Röt Formation, i.e. the surface adjacent to the underlying sandstones, the action of the largest forces would be expected, and thus the development of the most intense deformation, which is consistent with the observations. Such movements preferentially affect lithological changes. Moreover, such phenomena may have depended on the dip of the contemporary palaeoslope. According to Peel (2014), a regional slope

reaching 4° may result in gravitational sediment shifting, resulting in distinct modes of gravity-driven deformation, with 48% attributed to spreading and 52% to gliding. On steeper slopes, the contribution of gliding is larger, and vice versa. Such a phenomenon should cause sediment wasting in one place and aggradation in another. No such relationship was found based on the observations. Thus, it is now necessary to exclude the present hypothesis as a mechanism for the development of the deformation structures described.

Another event that could theoretically contribute to similar deformation is gravitational collapse caused by the dissolution of underlying strata, such as halite, gypsum or anhydrite. Such phenomena have been described by Stanton (1966), Beales and Hardy (1980), Morrow (1982), Babel (1991) and Friedman (1997). However, in such cases different types of breccia with a smaller contribution of other deformation structures should occur. The structures studied herein include breccias only in individual cases. Moreover, the breccia sizes exceed the drill core outline and usually accompany large-scale tectonic structures (Fig. 13E). Their origin may be associated with faults of local or regional scale, that probably formed during the Alpine orogeny. Beyond that, the sulphate intervals found in the succession of the Röt Formation are located above a continuous level with deformation, i.e. at least several to tens of metres above the base of the Röt Formation. If gypsum or anhydrite were to be partially or completely dissolved, then the breccia and other deformation structures should occur within or above such intervals. There is no evidence of sulphates or chlorides below the main deformed level in the NSS (Lower and Middle Buntsandstein/Röt Formation boundary). Similarly, no sulphates/chlorides or signs of sulphate/chlorides occurrence, such as casts after gypsum/halite crystals or imprints of gypsum/halite crystals, have been found at the base of the Röt Formation itself.

The most likely reason for the formation of the deformation structures described are earthquakes occurring during the sedimentation of the Röt Formation. In favour of this hypothesis, the following evidence may be adduced:

- the separation of the deformed levels by non-deformed levels (*sandwiched-like*),
- the large extent and repetition of the occurrence of deformation structures in the vertical profile,
- the large variability of the deformation types,
- the occurrence of the deformation structures throughout the study area,
- the occurrence of analogous structures in the Middle Triassic of the Silesian–Kraków and Holy Cross Mts. areas (Szulc et al., 2015; Matysik and Szulc, 2019).

The source of earthquakes could have been the faults surrounding the tectonic structure located in the area of today's Fore-Sudetic Block. Already during the sedimentation of the Permian and Zechstein, Sokółowski (1967), Milewicz (1977) and Bałazińska and Bossowski (1979) advocated the presence of such a structure and associated tectonic activity in the North Sudetic Synclinorium. Thus, it cannot be excluded that in the Early/Middle Triassic a reactivation of these tectonic structures took place, accompanied by earthquakes.

According to Szulc (2000), Narkiewicz and Szulc (2004), Szulc et al. (2015) and Matysik and Szulc (2019), seismic phenomena are not unique to the North Sudetic Synclinorium. Thus, the processes were of regional character. The basic difference between the phenomena described by the listed authors is that the deformation structures are present in the Silesia-Cracow and Holy Cross Mts. areas in the Middle Triassic. In this report, they occur in the uppermost part of the Lower Triassic, making them older.

## CONCLUSIONS

The data analysed provide evidence for tectonic activity and its influence on the study area during the sedimentation of the Röt Formation. From the common occurrence of deformation structures in the lowermost part of the Röt Formation and their sporadic presence in its upper parts, it can be concluded that tectonic activity was most intense during the beginning of the sedimentation of the Röt Formation. Later, the seismic activity declined, to disappear completely during the Muschelkalk deposition. The seismic activity probably involved movement on faults surrounding the structural element of the present-day Fore-Sudetic Block and that caused tectonic reassembly of the study area.

Summing up, it may be concluded that:

- the deformation was syn-sedimentary and early post-sedimentary;
- the largest accumulation of brittle and soft-sediment deformation structures occurs in the lowermost part of the

Röt Formation; these phenomena gradually disappear upwards;

- brittle deformations co-occur with soft-sediment deformation structures and are genetically linked;
- the largest accumulation of brittle and soft-sediment deformation structures occurs below sulphate deposits;
- local and regional faults observed in the Lower Triassic strata (Fig. 6) may have been responsible for the development of the deformation structures described.

**Acknowledgements.** Author would like to thank the GQ reviewers K. Jewuła (Ph.D. Research Assistant at Polish Academy of Sciences) and A. Becker (Państwowy Instytut Geologiczny) for their critical reading and valuable comments. Author would also thank to K. Mastalerz for his critical reading, discussions and inspiring suggestions during the preparation of the paper and also A. Kowalski for discussions and inspiring suggestions. The author would like to thank KGHM Polska Miedz S.A. for providing the material for the research.

## REFERENCES

- Alfaro, P., Gibert, L., Moretti, M., García-Tortosa, F.J., Sanz de Galdeano, C., Jesús Galindo-Zaldívar, J., Lopez-Garrido, A.C., 2010.** The significance of giant seismites in the Plio-Pleistocene Baza palaeo-lake (S Spain). *Terra Nova*, **22**:172–179.
- Allen, J.R.L., 1982.** Sedimentary Structures: their Character and Physical Basis. Developments in Sedimentology, **30** (Part B).
- Allen, J.R.L., 1986.** Earthquake magnitude-frequency epicentral distance and soft-sediment deformation in sedimentary basins. *Sedimentary Geology*, **46**: 67–75.
- Allen, J.R.L., Banks, N.L., 1972.** An interpretation and analysis of recumbent-folded deformed cross-bedding. *Sedimentology*, **19**: 257–283.
- Amit, R., Harrison, J.B.J., Enzel, Y., 1995.** Use of soils and colluvial deposits in analyzing tectonic events – the southern Arava valley, Israel. *Geomorphology*, **12**: 91–107.
- Anketell, J.M., Cegła, J., Dżułyński, S., 1970.** On the deformational structures in systems with reversed density gradients. *Rocznik Polskiego Towarzystwa Geologicznego*, **40**: 1–30.
- Assmann, P., 1944.** Die Stratigraphie der oberschlesischen Trias. Teil II – der Muschelkalk. *Abhandlungen des Reichsamts für Bodenforschung*, **208**: 1–124.
- Bąbel, M., 1991.** Dissolution of halite within the Middle Miocene (Badenian) laminated gypsum of southern Poland. *Acta Geologica Polonica*, **41**: 165–182.
- Bachmann, G.H., Geluk M.C., Warrington, G., Becker-Roman, A., Beutler, G., Hagdorn, H., Hounslow, M.W., Nitsch, E., Röhling, H.-G., Simon, T., Szulc, A., 2010.** Triassic. In: *Petroleum Geological Atlas of the Southern Permian Basin Area* (eds. J.C. Doornenbal and A.G. Stevenson): 149–173. EAGE Publications b.v., Houten.
- Bałazińska, J., Bossowski, A., 1979.** Internal geological structure of the central and western part of the North-Sudetic Synclinorium in light of new data (in Polish with English summary). *Geological Quarterly*, **23**: 309–322.
- Beales, F.W., Hardy, J.L., 1980.** Criteria for recognition of diverse dolomite types with an emphasis on studies on host rocks Mississippi Valley-type ore deposits. *SEPM Special Publication*, **28**: 197–213.
- Belzyt, S., Pisarska-Jamroży, M., 2017.** How to study seismites? A review of research methods (in Polish with English summary), *Acta Geographica Lodziensia*, **106**: 171–180.
- Casagrande, A., 1976.** Liquefaction and cyclic deformation of sands: a critical review. *Harvard Soil Mechanics Series*, **88**: 1–26.
- Chrzastek, A., 2002.** Stratigraphy and sedimentary conditions of the Röt and Lower Muschelkalk in the North Sudetic Basin (in Polish with English summary). *Prace Geologiczno-Mineralogiczne*, **73**: 1–178.
- Chrzastek, A., Wojewoda, J., 2011.** Mesozoic of SW Poland (North Sudetic Synclinorium) (in Polish with English summary). *Mezozoik i Kenozoik Dolnego Śląska LXXXI Zjazdu Polskiego Towarzystwa Geologicznego*, Wyd. Wind, Wrocław.
- Cohen, K.M., Finney, S.C., Gibbard, P.L., Fan, J.-X., 2013.** The ICS International Chronostratigraphic Chart. *Episodes*, **36**: 199–204.
- Collinson, J.D., Mountney, N. & Thompson, D., 2006.** *Sedimentary Structures*. Terra Publishing, London: 1–292.
- Cymerman, A., 1998.** Młodoalpejskie fałdy w depresji północnosudeckiej: przykłady z wapienia muszlowego z Raciborowic (in Polish). *Przegląd Geologiczny*, **46**: 348–354.
- Dadlez, R., Marek, S., Pokorski, J., Buła, Z., 2000.** Geological map of Poland without Cainozoic deposits 1:1 000 000. Państwowy Instytut Geologiczny.
- Dezes, P., Schmid, S.M., Ziegler, P.A., 2004.** Evolution of the European Cenozoic Rift System: interaction of the Alpine and Pyrenean orogens with their foreland lithosphere. *Tectonophysics*, **389**: 1–33.
- Durkowski, K., Sokalski, D., Wojewoda, J., 2017.** Pre- and post-consolidated sediment deformations in the Transitional Terrigenous Series PZt (Zechstein/Lower Buntsandstein) in the Grodziec Syncline, Sudetes: process interpretation and regional implications (in Polish with English summary). *Biuletyn Państwowego Instytutu Geologicznego*, **469**: 155–176.
- Fijałkowska-Mader, A., Durkowski, D., Sokalski, A., 2018.** Palynological and lithofacial implications for Zechstein stratigraphy in the marginal part of the North-Sudetic Synclinorium (Lower Silesia, southwestern Poland). *Zeitschrift der Deutschen Gesellschaft für Geowissenschaften*, **169**: 495–515.
- Folk, R.L., 1959.** Practical petrographic classification of limestones. *AAPG Bulletin*, **43**: 1–38.
- Fossen, H., 2010.** *Structural Geology*. Cambridge University Press, Cambridge.

- Friedman, G. M., 1997.** Dissolution-collapse breccias and paleokarst resulting from dissolution of evaporite rocks, especially sulfates. *Carbonates and Evaporites*, **12**: 53–63.
- Głuszyński, A., Aleksandrowski, P., 2021.** Late Cretaceous – Early Palaeogene inversion-related tectonic structures at the NE margin of the Bohemian Massif (SW Poland and northern Czechia). *Solid Earth Discuss.*
- Głuszyński, A., Bobek, K., Roman, M., 2019.** Reinterpretacja danych sejsmicznych 2D oraz model rozwoju strukturalnego w rejonie synkliny Bolesławca (synklinorium północnosudeckie) (in Polish). W ramach projektu statutowego nr M/18/0007: „Odtworzenie układu naprężeń i rozwoju strukturalnego synklinorium północnosudeckiego w okresie perm-kreda”. Archiwum KGHM Cuprum CB-R Sp. z o.o.: 68–79.
- Gradziński, R., Kostecka, A., Radomski, A., Unrug, R., 1986.** Zarys sedymentologii (in Polish). Wyd. Geol., Warszawa.
- Haakon, F., 2010.** *Structural Geology*. Cambridge University Press, Cambridge.
- Hampton, M.A., Lee, H.J., Locat, J., 1996.** Submarine landslides. *Reviews of Geophysics*, **34**: 33–59.
- Hielscher, P., Hartsch, J., 2010.** 3D Modelling of the Kupferschiefer area in Poland and Germany. Presentation on the Malta Workshop of the ProMine research project, EC 7th Frame Programme, CP-ProMine FP7-NMP-2008-LARGE-2
- Kämpf, H., Bankwitz, P., Strauch, G., Stiehl, G., Geisler, M., Gerstenberger, H., Haase, G., Klemm, W., Thomas, R., Vogler, P., 1985.** Local and regional processes and zoning in a hydrothermal Late Variscan vein mineralization from the southern part of the G.D.R. *Gerlands Beiträge zur Geophysik*, Leipzig, **94**: 426–434.
- Kastens, K.A., 1984.** Earthquakes as a triggering mechanism for debris flows and turbidites on the Calabrian Ridge. *Marine Geology*, **55**: 13–33.
- Kirkland, D.W., Anderson, R.Y., 1970.** Microfolding in the Castile and Toddlito Evaporites, Texas and New Mexico. *GSA Bulletin*, **81**: 3259–3282.
- Kirkland, D.W., Denison, R.E., Dean, W.E., 2000.** Parent brine of the Castile Evaporites (Upper Permian), Texas and New Mexico. *Journal of Sedimentary Research*, **70**: 749–761.
- Kowalski, A., Durkowski, K., Raczynski, P., 2018.** Zechstein marine deposits in the Wleń Graben (North Sudetic Synclinorium, SW Poland) – new insights into the paleogeography of the southern part of the Polish Zechstein Basin. *Annales Societatis Geologorum Poloniae*, **88**: 321–339.
- Krasoń, J., 1967.** Permian of the Bolesławiec Syncline (in Polish with English summary). *Prace Wrocławskiego Towarzystwa Naukowego*, **137**: 1–154.
- Kuenen, P.H., 1965.** Value of experiments in geology. *Geologie en Mijnbouw*, **44**: 22–36.
- Labaupe, P., Carrio-Schaffhauser, E., Gamond, J.-F., Renard, F., 2004.** Deformation mechanisms and fluid-driven mass transfers in the recent fault zones of the Corinth Rift (Greece). *C. R. Geoscience*, **336**: 375–383.
- Leeder, M.R., 1999.** *Sedimentology and Sedimentary Basins: from Turbulence to Tectonics*. Blackwell Science, Oxford.
- Leśniak, T., 1978.** Profil litostratygraficzny utworów retu i wapienia muszlowego w depresji północnosudeckiej (in Polish). *Geologia, Zeszyty Naukowe AGH*, **4**: 6–26.
- Leśniak, T.C., 1979.** Tectonics of the area between Raciborowice and Łaziska in north-eastern part of the North-Sudetic Depression (in Polish with English summary). *Geologia, Zeszyty Naukowe AGH*, **4**: 29–43.
- Lowe, D.R., 1975.** Water escape structures in coarse-grained deposits. *Sedimentology*, **22**: 157–204.
- Maltman, A., 1984.** On the term soft-sediment deformation. *Journal of Structural Geology*, **6**: 589–592.
- Maltman, A.J., 1994b.** Introduction and overview. In: *The Geological Deformation of Sediments* (ed. A.J. Maltman): 1–35. Chapman & Hall, London.
- Masson, D.G., Harbitz, C.B., Wynn, R.B., Pedersen, G., Lvholt, F., 2006.** Submarine landslides: processes, triggers and hazard prediction. *Philosophical Transactions of the Royal Society A: Mathematical, Physical and Engineering Sciences*, **364**: 2009–2039.
- Matysik, M., Szulc, J., 2019.** Shallow-marine carbonate sedimentation in a tectonically mobile basin, the Muschelkalk (Middle Triassic) of Upper Silesia (southern Poland). *Marine and Petroleum Geology*, **107**: 99–115.
- Matyszkiewicz, J., Krajewski, M., Kochman, A., Kozłowski, A., Duliński, M., 2016.** Oxfordian neptunian dykes with brachiopods from the southern part of the Kraków-Częstochowa Upland (southern Poland) and their links to hydrothermal vents. *Facies*, **62**: 1–28.
- McCalpin, J.P., Nelson, A.R., 2009.** Introduction to Paleoseismology. In: *Paleoseismology* (ed. J.P. McCalpin): 1–25. Elsevier, New York.
- Milewicz, J., 1962.** Uwagi o recie południowej części niecki północnosudeckiej (in Polish). *Przegląd Geologiczny*, **7**: 364–365.
- Milewicz, J., 1968.** The geological structure of the North-Sudetic Depression (in Polish with English summary). *Biuletyn Instytutu Geologicznego*, **227**: 5–27.
- Milewicz, J., 1971.** Relation between the North-Sudetic and East-Brandenburg Cretaceous formations (in Polish with English summary). *Geological Quarterly*, **15**: 122–136.
- Milewicz, J., 1976.** Rotliegendes in the vicinity of the Fore-Sudetic Block (in Polish with English summary). *Geological Quarterly*, **20**: 81–95.
- Milewicz, J., 1977.** A contribution to understanding the tectonic structure of the NW part of the North Sudetic Synclinorium (in Polish with English summary). *Acta Universitatis Wratislaviensis, Prace Geologiczno-Mineralogiczne VI*, **378**: 75–85.
- Milewicz, J., 1985.** Proposal of a formal stratigraphic scheme for deposits infilling the North Sudetic Basin (in Polish with English summary). *Przegląd Geologiczny*, **33**: 390–392.
- Miluk, A., Paletko, G., Sito, Ł., Targosz, P., 2016.** Dokumentacja z prac geofizycznych metodą sejsmiki refleksyjnej 2D w ramach tematu „Kompleksowa obsługa geologiczna projektów Synklina Grodziecka i Konrad” (in Polish). Kraków.
- Moretti, M., Van Loon, A.J., 2014.** Restrictions to the application of “diagnostic” criteria for recognizing ancient seismites. *Journal of Palaeogeography*, **3**: 162–173.
- Morrow, D.W., 1982.** Descriptive field classification of sedimentary and diagenetic breccia fabrics in carbonate rocks. *Bulletin of Canadian Petroleum Geology*, **30**: 227–229
- Mroczkowski, J., 1972.** Sedimentation of the Bunter in the North-Sudetic Basin (in Polish with English summary). *Acta Geologica Polonica*, **22**: 351–377.
- Narkiewicz, K., Szulc, J., 2004.** Controls on migration of conodont fauna in peripheral oceanic areas. An example from the Middle Triassic of the Northern Peri-Tethys. *Geobios*, **37**: 425–436.
- Oberc, J., 1972.** Budowa geologiczna Polski – Sudety i obszary przyległe (in Polish). Instytut Geologiczny. Budowa Geologiczna Polski, IV (2).
- Owen, G., Moretti, M., 2008.** Determining the origin of soft-sediment deformation structures: a case study from Upper Carboniferous delta deposits in south-west Wales, UK. *Terra Nova*, **20**: 237–245.
- Papadopoulos, G.A., Lefkopoulos, G., 1993.** Magnitude-distance relation for liquefaction in soil from earthquakes. *Bulletin of the Seismological Society of America*, **83**: 925–938.
- Peel, F.J., 2014.** The engines of gravity-driven movement on passive margins: quantifying the relative contribution of spreading vs. gravity sliding mechanisms. *Tectonophysics*, **633**: 126–142.
- Petrovic, A., Aigner, T., 2017.** Are shoal reservoirs discrete bodies? A coquina shoal outcrop analogue from the mid Triassic Upper Muschelkalk, SW Germany. *Journal of Petroleum Geology*, **40**: 249–275
- Potter, P.E., Pettijohn, F.J., 1963.** *Palaeocurrents and Basin Analysis*. Springer.
- Raczynski, P., Kurowski, L., Mastalerz, K., 1998.** Litostratygrafia i ewolucja basenu północnosudeckiego na przełomie paleozoiku

- i mezozoiku (in Polish). *Ekologiczne Aspekty Sedymentologii*, **1**: 75–100. WIND – J. Wojewoda, Wrocław.
- Rodríguez-Lopez, J.P., Meléndez, N., Soria, A.R., Liesa, C.L., Van Loon, A.J., 2007.** Lateral variability of ancient seismites related to differences in sedimentary facies (the syn-rift Escucha Formation, Mid-Cretaceous, Spain). *Sedimentary Geology*, **201**: 461–484.
- Rupke, N.A., 1978:** Deep clastic seas. In: *Sedimentary Environments and Facies* (ed. H.G. Reading): 372–415. Blackwell, Oxford.
- Scupin, H., 1933:** Der Buntsandstein der Nordsudeten. *Zeitschrift der Deutschen Geologischen Gesellschaft*, **85**: 161–189.
- Seilacher, A., 1969.** Fault-graded beds interpreted as seismites. *Sedimentology*, **13**: 155–159.
- Seilacher, A., 1984.** Sedimentary structures tentatively attributed to seismic events. *Marine Geology*, **55**: 1–12.
- Senkowiczowa, H., 1992.** Boundary between the upper Buntsandstein – Roeth and Muschelkalk in SW Poland (in Polish with English summary). *Przegląd Geologiczny*, **40**: 305–308.
- Shanmugam, G., 2016.** The seismite problem. *Journal of Palaeogeography*, **5**: 318–362.
- Sibson, R.H., Mcmoore, J.M., Rankin, A.H., 1975.** Seismic pumping — a hydrothermal fluid transport mechanism. *Journal of the Geological Society*, **131**: 653–659.
- Śliwiński, W., Raczyński, P., Wojewoda, J., 2003.** Sedymentacja utworów epiwaryscyjskiej pokrywy osadowej w basenie północnosudeckim (in Polish). *Przewodnik LXXIV Zjazdu PTG. Wycieczka 1*: 10–17.
- Sloss, L.L., Krumbein, W.C., Dapples, E.C., 1949.** Sedimentary facies in geologic history. Integrated facies analysis. *GSA Memoir*, **39**: 91–123.
- Smart, P.L., Palmer, R.J., Whitaker, F., Wright, V.P., 1988.** Neptunian dikes and fissure fills: an overview and account of some modern examples. In: *Paleokarst* (eds. N.P. James and P.W. Choquette): 149–163. Springer.
- Sokołowski, J., 1967.** Geological and structural characteristics of the Fore-Sudetic area (in Polish with English summary). *Geologia Sudetica*, **3**: 297–357.
- Solecki, A., 1994.** Tectonics of the North Sudetic Synclinorium. *Acta Universitatis Wratislaviensis* (1618), *Prace Geologiczno-Mineralogiczne*, **45**: 1–60.
- Solecki, A.T., 2011.** Structural evolution of the epi-Variscan platform cover in the North Sudetic Synclinorium (in Polish with English summary). *LXXXI Zjazd Polskiego Towarzystwa Geologicznego: Mezozoik i Kenozoik Dolnego Śląska – Żagań*: 1–10.
- Stanton, T.J.J., 1966.** The solution brecciation process. *GSA Bulletin*, **77**: 843–848.
- Szulc, J., 2000.** Middle Triassic evolution of the northern Peri-Tethys area as influenced by early opening of the Tethys Ocean. *Annales Societatis Geologorum Poloniae*, **70**: 1–48.
- Szulc, J., Becker, A., Mader, A., 2015.** Perm i trias – nowe otwarcie w historii Gór Świętokrzyskich (in Polish). *LXXXIV Zjazd Naukowy Polskiego Towarzystwa Geologicznego, Chęciny, Ekstensja i inwersja powaryscyjskich basenów sedymentacyjnych*. Państwowy Instytut Geologiczny, Warszawa: 11–27.
- Szyperko-Teller, A., Moryc, A., 1988.** Evolution of the Buntsandstein sedimentary basin in Poland (in Polish with English summary). *Geological Quarterly*, **32**: 53–72.
- Van der Pluijm, B.A., Marshak, S., 2004.** *Earth Structure: An Introduction to Structural Geology and Tectonics*. W. W. Norton & Company, Inc.
- Waldron, J.W.F., Gagnon, J.-F., 2011.** Recognizing soft-sediment structures in deformed rocks of orogens. *Journal of Structural Geology*, **33**: 271–279.
- Wallace, R., 1984.** Fault scarps formed during the earthquakes of October 2, 1915, Pleasant Valley, Nevada, and some tectonic implications. *U.S.G.S. Professional Paper*, **1274-A**.
- Wojewoda, J., 1987.** Seismotectonic deposits and structures in the Cretaceous sandstones of the intra-sudetic basin (in Polish with English summary). *Przegląd Geologiczny*, **35**: 169–175.
- Wojewoda, J., 2008.** Diffusional cells – an example of differentiated rheological reaction of granular sediment to seismic shock (in Polish with English summary). *Przegląd Geologiczny*, **56**: 842–847.
- Wojewoda, J., Burliga, S., 2008.** Clastic dykes and seismotectonic breccia in Permian deposits of the Nachod Basin (Middle Sudetes) (in Polish with English summary). *Przegląd Geologiczny*, **56**: 857–862.
- Wojewoda, J., Mastalerz, K., 1989.** Climate evolution, allocyclic and autocyclic sedimentation on the side of the Upper Carboniferous and Permian continental sediments in the Sudetes (in Polish with English summary). *Przegląd Geologiczny*, **37**: 173–180.
- Wojewoda, J., Rauch, M., Kowalski, A., 2016.** Synsedimentary seismotectonic features in Triassic and Cretaceous sediments of the Intrasudetic Basin (U Devěti krížů locality) – regional implications. *Geological Quarterly*, **60**: 355–364.
- Żelaźniewicz, A., Aleksandrowski, P., 2008:** Tectonic subdivision of Poland: southwestern Poland (in Polish with English summary). *Przegląd Geologiczny*, **56**: 904–911.
- Żelaźniewicz, A., Aleksandrowski, P., Buła, Z., Karnkowski, P., H., Konon, A., Oszczytko, N., Ślącza, A., Żaba, J., Żytko, K., 2011.** Regionalizacja geologiczna Polski (in Polish). *Komitet Nauk Geologicznych PAN, Wrocław*, **60**: 1–62.